INTERNATIONAL JOURNAL OF ROBUST AND NONLINEAR CONTROL
Int. J. Robust Nonlinear Control 2009; **19**:986–1015
Published online 22 July 2008 in Wiley InterScience (www.interscience.wiley.com). DOI: 10.1002/rnc.1358

A test for stability robustness of linear time-varying systems utilizing the linear time-invariant *v*-gap metric

Wynita M. Griggs[1,*,†], Alexander Lanzon[2] and Brian D. O. Anderson[1,3]

[1]*Department of Information Engineering, Research School of Information Sciences and Engineering, The Australian National University, Canberra, ACT 0200, Australia*
[2]*Control Systems Centre, School of Electrical and Electronic Engineering, University of Manchester, Sackville Street, Manchester M60 1QD, U.K.*
[3]*National ICT Australia Limited, Locked Bag 8001, Canberra, ACT 2601, Australia*

SUMMARY

A stability robustness test is developed for internally stable, nominal, linear time-invariant (LTI) feedback systems subject to structured, linear time-varying uncertainty. There exists (in the literature) a necessary and sufficient structured small gain condition that determines robust stability in such cases. In this paper, the structured small gain theorem is utilized to formulate a (sufficient) stability robustness condition in a scaled LTI *v*-gap metric framework. The scaled LTI *v*-gap metric stability condition is shown to be computable via linear matrix inequality techniques, similar to the structured small gain condition. Apart from a comparison with a generalized robust stability margin as the final part of the stability test, however, the solution algorithm implemented to test the scaled LTI *v*-gap metric stability robustness condition is shown to be independent of knowledge about the controller transfer function (as opposed to the LMI feasibility problem associated with the scaled small gain condition which is dependent on knowledge about the controller). Thus, given a nominal plant and a structured uncertainty set, the stability robustness condition presented in this paper provides a single constraint on a controller (in terms of a large enough generalized robust stability margin) that (sufficiently) guarantees to stabilize *all* plants in the uncertainty set. Copyright © 2008 John Wiley & Sons, Ltd.

Received 19 September 2007; Revised 31 May 2008; Accepted 31 May 2008

KEY WORDS: *v*-gap metric; stability robustness; structured uncertainty; linear time-varying uncertainty

*Correspondence to: Wynita M. Griggs, Department of Information Engineering, Research School of Information Sciences and Engineering, The Australian National University, Canberra, ACT 0200, Australia.
†E-mail: wynita.griggs@gmail.com

Contract/grant sponsor: ARC Discovery-Projects Grant; contract/grant number: DP0342683
Contract/grant sponsor: National ICT Australia

1. INTRODUCTION

When a stabilizing controller is designed for a nominal plant, a desired objective is that the controller also succeeds in stabilizing the 'true-life' system in the face of uncertainty. Uncertainty may be modeled as an unstructured perturbation to the nominal plant: classes of these uncertainties include additive uncertainty, input- or output-multiplicative uncertainty, and input- or output-feedback uncertainty. A structured uncertainty model may be used when plants are subjected to multiple uncertainties, for example,hen the plant contains multiple unstructured uncertainties or when the plant contains a number of uncertain parameters.

The problem discussed in this paper involves determining internal stability of a system subject to structured, linear time-varying (LTV) uncertainties, given that a nominal feedback interconnection, consisting of a linear time-invariant (LTI) system P_0 and an LTI controller K as shown in Figure 1, is internally stable. Often it is suitable to describe such a problem using a linear fractional transformation (LFT) framework, as shown in Figure 2, where $F(s)$ is a transfer function matrix that describes the relationship between the nominal LTI plant P_0 and the structured LTV uncertainty denoted by Δ.

This type of stability problem has been studied intensively in the literature. For instance, Boyd and Yang [1] reduced the problem (where Δ was possibly nonlinear) to a question of existence of a quadratic Lyapunov function of a certain structure. The existence of the Lyapunov function was determined by solving a convex optimization problem. In [2], where complex-valued uncertainty is considered, quadratic stability (which is related to the existence of quadratic Lyapunov functions) is shown to be equivalent to a scaled $\mathscr{H}_\infty$ norm condition when the structured uncertainty consists of only two diagonal blocks. (The equivalence for more than two blocks is not in general true [2].) A frequency-domain stability criterion based on integral quadratic constraints (IQCs)

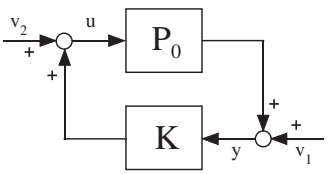

Figure 1. Nominal closed-loop system.

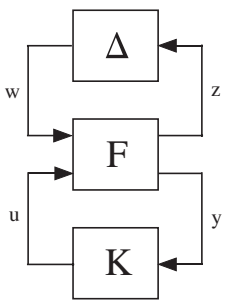

Figure 2. Robust stability problem.

DOI: 10.1002/rnc

was derived in [3], where an uncertainty structure consisting of bounded, real-valued, differentiable, time-varying parameters (with bounded derivatives) down the diagonal was considered. The paper [4] considered structured slowly time-varying uncertain gains and obtained a sufficient frequency-domain condition for stability when pairs of the uncertain gain and its derivative belonged to a given convex set. A sufficient stability condition (that can be formulated in terms of linear matrix inequalities (LMIs)) was derived in [5], and was shown to be less conservative than a standard scaled small gain stability condition when the uncertainty structure contains real, repeated, time-varying parameters (i.e. when sub-blocks of the uncertainty structure share the same scalars). Obtaining this condition did not require the use of IQCs [3], or the explicit construction of a quadratic Lyapunov function [2]; but followed from basic properties of the structured singular value [6–8] (although the results are closely related to notions of quadratic stability—[2] used the quadratic stability approach to derive the condition for the case where all of the parameters are complex). In [9], a computational approach was developed for designing a globally optimal controller that is robust to time-varying nonlinear perturbations in the plant. The controller design problem is formulated as an optimization with bilinear matrix inequality constraints, and solved to optimality by a branch-and-bound algorithm (see [10], for instance). A branch-and-bound scheme was also used in [11] to obtain a globally optimal solution to a robust synthesis problem.

The scaled small gain condition has remained a well-utilized tool in determining stability robustness [12–14]. Provided, as described above, that the nominal plant and controller are LTI, and the uncertainties are of a certain structured form, then this scaled small gain condition is necessary and sufficient [12, 13].

In this paper, we utilize the scaled small gain condition to develop a stability robustness test for problems of the sort shown in Figure 2 (where Δ is structured LTV uncertainty, and F and K are LTI). Particularly, we derive a (sufficient) stability robustness condition in a scaled LTI ν-gap metric framework and show that this condition can be checked via solving an LMI feasibility problem. The scaled small gain condition can be checked by solving an LMI feasibility problem too. The advantage of using the condition proposed in this paper, however, is that the LMI feasibility problem associated with the condition is independent of knowledge about the controller. Solution of the LMI feasibility problem (*independent of* K) provides a numerical quantity (which we shall loosely call the 'scaled LTI ν-gap quantity'); and the scaled LTI ν-gap quantity is then compared with a generalized robust stability margin, $b_{P_0,K}$ (which is dependent on K and on the nominal plant) [15–17]. Such a constraint could be very easily incorporated into a control design procedure. Unsurprisingly, the scaled LTI ν-gap metric condition may provide a more conservative test for stability robustness than the scaled small gain condition (since the less knowledge one utilizes regarding the controller, the more careful one has to be). However, given a collection of difficult (uncertain) plants, the scaled LTI ν-gap quantity (as opposed to the scaled small gain condition) gives immediate indication to the control system designer of what $b_{P_0,K}$ must be in order to (sufficiently) ensure stability robustness.

The LTI ν-gap metric was introduced in [18]. Similar to its predecessor gap metric [19–23], the ν-gap metric offers a measure of difference or 'distance' between two time-invariant systems from a feedback perspective, and thus provides a means of quantifying feedback system stability robustness. Any plant at a ν-gap distance less than, say β, from the nominal plant will be stabilized by any controller that stabilizes the nominal with a stability margin of at least β. Unlike the gap metric, it can also be said of the ν-gap metric that any plant at a distance greater than β from the nominal will be destabilized by some controller that stabilizes the nominal with a stability margin

DOI: 10.1002/rnc

of at least β [18]. In this sense, the LTI ν-gap metric is less conservative than the gap metric. The LTI ν-gap metric is also simpler to compute.

Time-varying and nonlinear extensions to both the gap metric [24–28] and the ν-gap metric [29–31] exist. Analytical computations of the metrics in these cases are generally not possible. For example, if we consider the calculation of the time-varying ν-gap metric defined by Anderson *et al.* [31, Definition III.4] between a single-input, single-output LTI plant

$$P_0 = \left(\begin{array}{c|c} -1 & 1 \\ \hline 1 & 0 \end{array}\right)$$

and the LTV output-multiplicatively perturbed plant

$$P_1 = \left(\begin{array}{c|c} -1 & 1 \\ \hline 1+\varepsilon \sin(at+b) & 0 \end{array}\right)$$

where $\varepsilon \in [0, 1]$, we see that, using [31, Definition III.4], one is required to solve differential Riccati equations to obtain time-varying normalized graph symbols. This is not analytically possible, even for the basic example mentioned. Despite the fact that we are concerned with LTV perturbations, however, we can still use effective ν-gap metric methods by showing the applicability of calculations for time-invariant problems to the time-varying case.

A description of the scaled small gain condition is provided in Section 2. A stability robustness condition in a scaled LTI ν-gap metric framework is derived in Section 3. The theoretical construction of the LMI feasibility problem as required for evaluation of the scaled LTI ν-gap quantity is given in Section 4; and a complete solution algorithm to test the scaled LTI ν-gap metric condition is provided in Section 5. An example of the implementation of the solution algorithm is provided in Section 6. Section 7 concludes the paper.

Preliminaries: The following is an account of the mathematical notation used throughout this paper. The space $\mathscr{L}_2(-\infty, \infty)$ is a space consisting of Lebesgue measurable functions with finite norm. $\mathscr{L}_2[0, \infty)$ is the subspace of $\mathscr{L}_2(-\infty, \infty)$ with functions zero for $t<0$. $\mathscr{R}$ denotes the set of proper real rational transfer function matrices. $\mathscr{L}_\infty(\mathrm{j}\mathbb{R})$ is a Banach space of matrix (or scalar)-valued functions that are essentially bounded on $\mathrm{j}\mathbb{R}$. The Hardy space $\mathscr{H}_\infty$ is the closed subspace of $\mathscr{L}_\infty$ with functions that are analytic and bounded in the open right-half plane (RHP), with norm denoted as $\|\cdot\|_\infty$. In other words, $\mathscr{H}_\infty$ is the space of transfer functions of stable, LTI, continuous-time systems. $\mathscr{R}\mathscr{H}_\infty$ denotes the subspace of $\mathscr{H}_\infty$ where transfer function matrices are proper and real rational. The $\mathscr{L}_2$-induced norm for LTV operators will be denoted by $\|\cdot\|$. For LTI systems, the $\mathscr{L}_2$-induced norm is precisely equal to $\|\cdot\|_\infty$.

For a general matrix $X = [x_{ij}] \in \mathbb{C}^{r\times s}$, X^* denotes the complex conjugate transpose $[\bar{x}_{ji}]$. For a transfer function matrix $X(s) \in \mathscr{R}^{r\times s}$, $X^\sim(s)$ is defined to mean $X(-s)^{\mathrm{T}}$, whereas $X(\mathrm{j}\omega)^*$ denotes the complex conjugate transpose of the frequency response function $X(\mathrm{j}\omega)$ at each frequency, i.e. $X(\mathrm{j}\omega)^* = X(-\mathrm{j}\omega)^{\mathrm{T}}$. Let $X \in \mathbb{C}^{(r_1+r_2)\times(s_1+s_2)}$ be partitioned as follows:

$$\begin{pmatrix} X_{11} & X_{12} \\ X_{21} & X_{22} \end{pmatrix}$$

and let $Y_\mathrm{l} \in \mathbb{C}^{s_2\times r_2}$ and $Y_\mathrm{u} \in \mathbb{C}^{s_1\times r_1}$. The notations

$$F_\mathrm{l}(X, Y_\mathrm{l}) := X_{11} + X_{12}Y_\mathrm{l}(I - X_{22}Y_\mathrm{l})^{-1}X_{21}$$

DOI: 10.1002/rnc

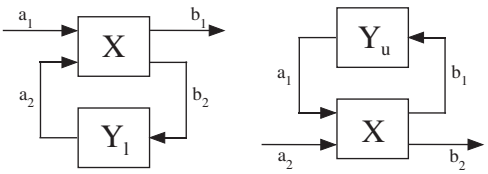

Figure 3. Lower and upper LFTs.

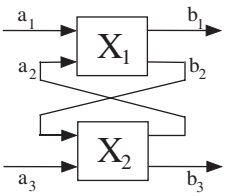

Figure 4. Redheffer star product.

and

$$F_{\mathrm{u}}(X, Y_{\mathrm{u}}) := X_{22} + X_{21} Y_{\mathrm{u}} (I - X_{11} Y_{\mathrm{u}})^{-1} X_{12}$$

refer to the standard lower and upper linear fractional representations, respectively, as shown in Figure 3. $X_1 \star X_2$ denotes the interconnection of two LFTs known as the Redheffer star product, as shown in Figure 4 [32, Section 10.4]. The notation

$$\left(\begin{array}{c|c} A & B \\ \hline C & D \end{array}\right)$$

refers to a system realization (A, B, C, D). Well posedness of closed loops is assumed throughout this paper.

2. THE SCALED SMALL GAIN CONDITION

A description of the scaled small gain condition of interest in this paper is provided as follows (see also [13]). Consider the uncertain system shown in Figure 2. Suppose that the generalized system F is partitioned as

$$F = \begin{pmatrix} F_{11} & F_{12} \\ F_{21} & F_{22} \end{pmatrix} \tag{1}$$

where $F_{11} \in \mathscr{R}^{p \times q}$, $F_{12} \in \mathscr{R}^{p \times m}$, $F_{21} \in \mathscr{R}^{n \times q}$, and $F_{22} \in \mathscr{R}^{n \times m}$. Furthermore, let a stabilizable and detectable realization for $F \in \mathscr{R}^{(p+n) \times (q+m)}$ be given by

$$\left(\begin{array}{c|cc} A & B_1 & B_2 \\ \hline C_1 & D_{11} & D_{12} \\ C_2 & D_{21} & 0 \end{array}\right) \tag{2}$$

DOI: 10.1002/rnc

Let the nominal plant be denoted by $P_0 := F_u(F, 0) = F_{22}$ and the controller be denoted by $K \in \mathscr{R}^{m\times n}$. Let the interconnection of P_0 and K, as shown in Figure 1, be denoted by $[P_0, K]$. This interconnection is said to be internally stable if it is well posed and each of the four transfer functions mapping the signals v_1 and v_2 to y and u are stable; that is, they belong to RH_∞ [32]. Recall that it is our intention to assume that this interconnection is indeed internally stable. Suppose that P_0 has an inherited realization (A, B_2, C_2) that is stabilizable and detectable. Then $[P_0, K]$ is internally stable if and only if the system shown in Figure 5 is *internally stable* (this taken to mean that the system is well posed and that each of the nine transfer functions mapping w, v_1 and v_2 to z, y and u are stable) [32, Lemma 12.2]. Denote $Z := F_l(F, K)$. The system in Figure 2 may be reduced to the system shown in Figure 6.

Let us define a block-diagonal uncertainty set

$$\mathbf{\Delta} := \{\Delta = \mathrm{diag}(\Delta_1 \ldots \Delta_k) : \Delta_i \text{ is a } q_i \times p_i \text{ causal LTV operator and } \|\Delta\| \leqslant 1\}$$

where $q := q_1 + \cdots + q_k$ and $p := p_1 + \cdots + p_k$. Here we make the observation that since $\mathbf{\Delta}$ is a subset of the unit ball of causal LTV operators, then clearly the standard small gain condition

$$\|Z\|_\infty < 1$$

for *unstructured* uncertainty is a sufficient test for input–output stability of the system shown in Figure 6 [13]. Now associate with $\mathbf{\Delta}$ a set of scalings that commute with the set of perturbations. In particular, we will choose a set of constant diagonal matrix pairs that share the same scalar coefficients, denoted as

$$\mathbf{D} := \{(D_l, D_r) : D_l = \mathrm{diag}(d_1 I_{q_1}, \ldots, d_k I_{q_k}),\ D_r = \mathrm{diag}(d_1 I_{p_1}, \ldots, d_k I_{p_k}),\ d_i \in \mathbb{R},\ d_i > 0\}$$

such that

$$\Delta = D_l \Delta D_r^{-1}$$

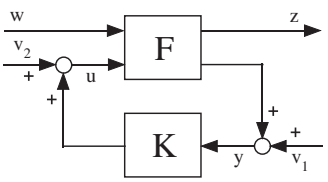

Figure 5. Internal stability of $F_l(F, K)$.

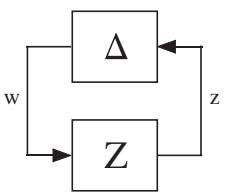

Figure 6. Reduced stability robustness problem.

DOI: 10.1002/rnc

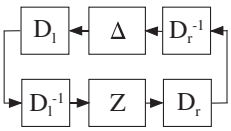

Figure 7. Scaled robust stability problem.

$\forall \Delta \in \mathbf{\Delta}$. Stability of the system in Figure 7 is equivalent to stability of the system in Figure 6 (since it is the same system). This means that if we can find an element $\widetilde{D} = (D_\mathrm{l}, D_\mathrm{r})$ of $\mathbf{D}$ satisfying

$$\| D_\mathrm{r} Z D_\mathrm{l}^{-1} \|_\infty < 1$$

then we can guarantee that the system in Figure 6 is input–output stable. Since the identity matrices (of suitable dimensions) are members of $\mathbf{D}$, there always exists a $\widetilde{D} = (D_\mathrm{l}, D_\mathrm{r}) \in \mathbf{D}$ such that $\| D_\mathrm{r} Z D_\mathrm{l}^{-1} \|_\infty \leqslant \| Z \|_\infty$. Thus, the scaled small gain condition provides a less conservative test for stability, then the standard small gain condition [13]. In fact, it is furthermore possible to obtain the following result [13].

Theorem 1 (*Dullerud and Paganini* [*13, Theorem 9.6*])
Consider a causal, LTI system with transfer function matrix $Z \in \mathscr{RH}_\infty$. The following are equivalent:

(i) The system in Figure 6 is stable for all $\Delta \in \mathbf{\Delta}$.
(ii) The inequality $\inf_{\widetilde{D} = (D_\mathrm{l}, D_\mathrm{r}) \in \mathbf{D}} \| D_\mathrm{r} Z D_\mathrm{l}^{-1} \|_\infty < 1$ holds.

The proof of Theorem 1 is provided in [13]. A discrete-time version of Theorem 1 can be found in [12, 14]. Note that there exist other cases in which the scaled small gain condition is necessary and sufficient condition for stability. Another case that will be utilized in this paper is where the uncertainties are LTI and structured such that they consist of two diagonal blocks. Reference [32, Chapter 11] provides thorough discussion of this case.

3. THE SCALED LTI ν-GAP METRIC CONDITION

Utilizing Theorem 1, we derive a stability robustness result for the system shown in Figure 2 in a scaled, LTI, ν-gap metric framework. The following is claimed: given that a controller K stabilizes a nominal plant P_0 with generalized robust stability margin $b_{P_0,K}$, if a certain LTI quantity (which is independent of K) is smaller than $b_{P_0,K}$, then the same controller will stabilize the system when subjected to structured LTV uncertainty. If the LTI quantity is equal to or larger than $b_{P_0,K}$, then the controller may or may not stabilize the system when subject to uncertainty.

Let $\boldsymbol{\delta} := \{\delta : \delta \in \mathscr{RH}_\infty^{q \times p}, \|\delta\|_\infty \leqslant 1\}$ and $\boldsymbol{\delta}_\mathbf{0} := \{\delta : \delta \in \mathscr{RH}_\infty^{q \times p}, \|\delta\|_\infty < 1\}$ denote full-block sets of LTI uncertainties. The generalized robust stability margin, $b_{P_0,K}$; the optimal generalized robust stability margin, $b_{\mathrm{opt}}(P_0) := \sup_K b_{P_0,K}$; and the LTI ν-gap metric, denoted as $\delta_\nu(P_0, P_1)$ where $P_0 \in \mathscr{R}^{n \times m}$ and $P_1 \in \mathscr{R}^{n \times m}$ are defined as in [17].

Theorem 2
Let a generalized plant $F \in \mathscr{R}^{(p+n) \times (q+m)}$ be partitioned as in (1) and have a stabilizable and detectable realization as given by (2). Let $P_0 := F_\mathrm{u}(F, 0)$ be the nominal plant with an inherited

DOI: 10.1002/rnc

realization (A, B_2, C_2) which is stabilizable and detectable[‡]; and let $K \in \mathscr{R}^{m\times n}$ be a stabilizing controller for P_0, with a given stabilizable and detectable realization. Consider the uncertainty sets $\mathbf{\Delta}$, $\boldsymbol{\delta}$ and $\boldsymbol{\delta}_\mathbf{0}$ and the set of constant diagonal matrix pairs $\mathbf{D}$ as defined above. Suppose that each $\Delta \in \mathbf{\Delta}$ and each $\delta \in \boldsymbol{\delta}$ has a given stabilizable and detectable realization; and that each induced realization[§] for $F_\mathrm{u}(F, \Delta)$ and $F_\mathrm{u}(F, D_\mathrm{l}^{-1}\delta D_\mathrm{r})$ is stabilizable and detectable (as defined in Theorem A2 of the Appendix). If

$$\inf_{\widetilde{D}=(D_\mathrm{l}, D_\mathrm{r})\in\mathbf{D}} \sup_{\delta\in\boldsymbol{\delta}_\mathbf{0}} \delta_\nu(P_0, F_\mathrm{u}(F, D_\mathrm{l}^{-1}\delta D_\mathrm{r})) < b_{P_0,K} \tag{3}$$

then $[P_{\mathrm{LTV}}, K]$ is internally stable for all $\Delta \in \mathbf{\Delta}$, where $P_{\mathrm{LTV}} := F_\mathrm{u}(F, \Delta)$.

Proof
We have

$$\inf_{\widetilde{D}=(D_\mathrm{l}, D_\mathrm{r})\in\mathbf{D}} \sup_{\delta\in\boldsymbol{\delta}_\mathbf{0}} \delta_\nu(P_0, F_\mathrm{u}(F, D_\mathrm{l}^{-1}\delta D_\mathrm{r})) < b_{P_0,K}$$

$$\Leftrightarrow \exists \widetilde{D} \in \mathbf{D} : \forall \delta \in \boldsymbol{\delta}\, \delta_\nu(P_0, F_\mathrm{u}(F, D_\mathrm{l}^{-1}\delta D_\mathrm{r})) < b_{P_0,K} \tag{4}$$

$$\Rightarrow \exists \widetilde{D} \in \mathbf{D} : \forall \delta \in \boldsymbol{\delta} \text{ the system in Figure 8 is internally stable (using the stability result associated with the LTI } \nu\text{-gap metric that is provided in [17, 18])} \tag{5}$$

$$\Leftrightarrow \exists \widetilde{D} \in \mathbf{D} : \| D_\mathrm{r} F_\mathrm{l}(F, K) D_\mathrm{l}^{-1} \|_\infty < 1 \text{ (using the small gain theorem in [32, Theorem 9.1], since } F_\mathrm{l}(F, K) \in \mathscr{RH}_\infty \text{ as shown in Appendix A.1)}$$

$$\Leftrightarrow \inf_{\widetilde{D}=(D_\mathrm{l}, D_\mathrm{r})\in\mathbf{D}} \| D_\mathrm{r} F_\mathrm{l}(F, K) D_\mathrm{l}^{-1} \|_\infty < 1$$

$$\Leftrightarrow \forall \Delta \in \mathbf{\Delta} \text{ the system in Figure 2 is internally stable (from Theorem 1)} \qquad \square$$

The only implication in the above proof that is not necessary and sufficient is the one that relates (4) to (5), which is based on [17, Remark 3.11]. Therefore, the scaled LTI ν-gap metric stability condition (3), even though only a sufficient condition, is still the strongest result one could derive in the following sense. The LTI ν-gap metric is strongly necessary in the sense that there always exists a controller K satisfying $\delta_\nu(\cdot,\cdot) \not< b_{P,K}$ for which internal stability is lost (see [18, Theorem 4.5; 17, Remark 3.11] for further details), and hence there always exists a K that does not satisfy inequality (3) for which robust internal stability of the system shown in Figure 8 is lost.

[‡]Such an assumption is a standard assumption in $\mathscr{H}_\infty$ control and is necessary and sufficient for F to be internally stabilizable via a controller connecting y to u [33].
[§]Induced realizations for upper LFTs are formally defined in the Appendix (see Definition A1).

DOI: 10.1002/rnc

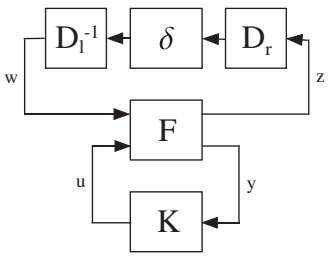

Figure 8. Internal stability of LTI system.

An observation in regard to the scaled small gain condition when compared with the scaled LTI ν-gap metric condition is as follows. The scaled small gain condition is: does there exist a $\widetilde{D}=(D_{\mathrm{l}}, D_{\mathrm{r}})\in\mathbf{D}$ such that

$$\|D_{\mathrm{r}}F_{\mathrm{l}}(F, K)D_{\mathrm{l}}^{-1}\|_{\infty}<1$$

can be tested directly using LMI techniques. Part (ii) of the following lemma shows that the condition is equivalent to a convex condition over the positive scaling set $\mathbf{D}$; and by part (iii) of the lemma, checking the condition reduces to solving an LMI feasibility problem [13].

Lemma 3 (*Dullerud and Paganini* [*13, Proposition 8.6*])
Suppose that $Z\in\mathscr{RH}_{\infty}$ with transfer function matrix $Z(s)=C(sI-A)^{-1}B+D$, and A is Hurwitz of order n. Then the following are equivalent:

(i) $\exists\widetilde{D}\in\mathbf{D}: \|D_{\mathrm{r}}ZD_{\mathrm{l}}^{-1}\|_{\infty}<1$;
(ii) $\exists\widetilde{D}\in\mathbf{D}: Z^{*}D_{\mathrm{r}}Z-D_{\mathrm{l}}<0$;
(iii) $\exists\widetilde{D}\in\mathbf{D}$ and a symmetric $n\times n$ matrix $X>0$ such that

$$\begin{pmatrix}C^{*}\\ D^{*}\end{pmatrix}D_{\mathrm{r}}(C\quad D)+\begin{pmatrix}A^{*}X+XA & XB\\ B^{*}X & -D_{\mathrm{l}}\end{pmatrix}<0$$

Refer to [13] for the proof. Note that testing the scaled small gain condition in this manner is dependent on information about the controller. That is, for each different K, one must solve a different LMI feasibility problem (for instance) to determine stability. The LHS of (3), however, is independent of K. In the remainder of this paper, it will be shown that this 'scaled LTI ν-gap' quantity on the LHS of (3) can also be computed by solving an LMI feasibility problem (in association with a bisectional search). Since the quantity on the LHS of (3) is independent of K, this means that the (entire solution algorithm involving the) associated LMI feasibility problem has to be solved only once (given F); the quantity is then compared with $b_{P_0,K}$, which is computed as required. The scaled LTI ν-gap metric condition may provide a more conservative test for stability robustness than the scaled small gain condition (since the less knowledge one utilizes regarding the controller, the more careful one has to be). However, given a collection of difficult (uncertain) plants, the scaled LTI ν-gap metric condition (as opposed to the scaled small gain condition) provides a single constraint on a controller (in terms of a large enough generalized robust stability margin) that (sufficiently) guarantees to stabilize *all* plants in the uncertainty set. A constraint such as this could very easily be incorporated into a control design procedure.

DOI: 10.1002/rnc

4. AN LMI FEASIBILITY PROBLEM

It was stated above that the LTI quantity on the LHS of (3) can be computed via solving an LMI feasibility problem. This result is presented later in this section (see Theorem 7). First, some preliminary results are required.

The first result is a minor but important extension of [34, Proposition 1.1], and relates an LTI ν-gap metric and a transfer function matrix stability and small gain concept. First, an LTI system $\tilde{R}$ (dependent on some strictly proper[¶] LTI system $P_1 \in \mathscr{R}^{n\times m}$ and some number $\beta \in (0, b_{\text{opt}}(P_1))$) is introduced as follows. Suppose that P_1 has a stabilizable and detectable realization $(A_{P_1}, B_{P_1}, C_{P_1})$. Let $X = X^* \geqslant 0$ be the stabilizing solution to the generalized control algebraic Riccati equation

$$A_{P_1}^* X + X A_{P_1} - X B_{P_1} B_{P_1}^* X + C_{P_1}^* C_{P_1} = 0$$

and $Z = Z^* \geqslant 0$ be the stabilizing solution to the generalized filtering algebraic Riccati equation

$$A_{P_1} Z + Z A_{P_1}^* - Z C_{P_1}^* C_{P_1} Z + B_{P_1} B_{P_1}^* = 0$$

Let $\gamma := 1/\beta$. Define, as per [35], a transfer function matrix $\tilde{R} \in \mathscr{R}^{(n+m)\times(m+n)}$ via the realization

$$\left(\begin{array}{c|cc} A_{\tilde{R}} & B_{\tilde{R}_1} & B_{\tilde{R}_2} \\ \hline C_{\tilde{R}_1} & 0 & I \\ C_{\tilde{R}_2} & \sqrt{\gamma^2 - 1}\, I & 0 \end{array}\right) \tag{6}$$

where $Y := (1/(\gamma^2 - 1))Z$, $\bar{Y} := Y(I - XY)^{-1}$ and

$$A_{\tilde{R}} := A_{P_1} - B_{P_1} B_{P_1}^* X - \gamma^2 \bar{Y} C_{P_1}^* C_{P_1}$$

$$B_{\tilde{R}_1} := \frac{\gamma}{\sqrt{\gamma^2 - 1}} (I - YX)^{-1} B_{P_1}$$

$$B_{\tilde{R}_2} := \gamma \bar{Y} C_{P_1}^*$$

$$C_{\tilde{R}_1} := -\gamma C_{P_1}$$

$$C_{\tilde{R}_2} := -\gamma B_{P_1}^* X$$

[¶] P_1 is assumed to be strictly proper for simplicity in [35]. It is quite satisfactory for us to consider also a strictly proper P_1 because this material is to be applied to subsequent results where a generalized system F with a realization given as in (2), and a nominal system P_0 with an inherited realization (A, B_2, C_2) are considered.

DOI: 10.1002/rnc

Note it was shown in [36] that $\tilde{R}$ is invertible in $\mathscr{R}^{(m+n)\times(n+m)}$. In fact, $\tilde{R}$ in this paper is equivalent to R^{-1} in [34–36], where

$$R := \left(\begin{array}{c|cc} A_{P_1}+\dfrac{1}{\gamma^2-1}B_{P_1}B_{P_1}^*X+\dfrac{\gamma^2}{\gamma^2-1}\bar{Y}X^*B_{P_1}B_{P_1}^*X & B_{\tilde{R}_2} & \dfrac{\gamma}{\gamma^2-1}(I+\bar{Y}X^*)B_{P_1} \\ \hline -\dfrac{1}{\sqrt{\gamma^2-1}}C_{\tilde{R}_2} & 0 & \dfrac{1}{\sqrt{\gamma^2-1}}I \\ -C_{\tilde{R}_1} & I & 0 \end{array}\right)$$

It was also shown in [36] that $(R_{12})^{-1}, (R_{21})^{-1} \in \mathscr{RH}_\infty$; and it was noted in [37] that the realization for R was naturally induced by the problem structure described in [34–37].

Realization (6) is stabilizable and detectable since there exist matrices

$$F_{\tilde{R}} := \begin{pmatrix} 0 \\ -C_{\tilde{R}_1} \end{pmatrix} \quad \text{and} \quad L_{\tilde{R}} := (-B_{\tilde{R}_2} \;\; 0)$$

such that

$$A_{\tilde{R}}+(B_{\tilde{R}_1} \;\; B_{\tilde{R}_2})F_{\tilde{R}} \quad \text{and} \quad A_{\tilde{R}}+L_{\tilde{R}}\begin{pmatrix} C_{\tilde{R}_1} \\ C_{\tilde{R}_2} \end{pmatrix}$$

respectively, are Hurwitz.[‖] The extension to [34, Proposition 1.1] is as follows:

Lemma 4
Given two LTI systems P_1, $P_2 \in \mathscr{R}^{n\times m}$, where P_1 is strictly proper (see Footnote ¶) but P_2 is not necessarily strictly proper, and a number $\beta \in (0, b_{\text{opt}}(P_1))$, define an LTI system $\tilde{R}$ (dependent on P_1 and β) as above. Then

$$\begin{gathered} \delta_\nu(P_1, P_2) \leqslant \beta \\ \Updownarrow \\ \|F_l(\tilde{R}, P_2)\|_\infty \leqslant 1 \text{ and the system in Figure 9 is internally stable} \end{gathered} \tag{7}$$

Proof
The difference between the statement of Lemma 4 and the statement of [34, Proposition 1.1] occurs at (7). In [34, Proposition 1.1], this condition reads

$$\|F_l(\tilde{R}, P_2)\|_\infty \leqslant 1 \quad \text{and} \quad F_l(\tilde{R}, P_2) \in \mathscr{RH}_\infty$$

whereas in Lemma 4, this condition reads

$$\|F_l(\tilde{R}, P_2)\|_\infty \leqslant 1 \text{ and the system in Figure 9 is internally stable}$$

Hence, the aim of the proof is to establish that $F_l(\tilde{R}, P_2) \in \mathscr{RH}_\infty$ if and only if the system in Figure 9 is internally stable.

[‖]Note that $A_{\tilde{R}} - B_{\tilde{R}_2}C_{\tilde{R}_1} = A_{P_1} - B_{P_1}B_{P_1}^*X$.

DOI: 10.1002/rnc

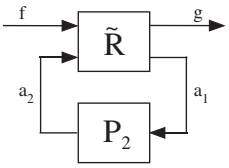

Figure 9. Internal stability of $F_1(\tilde{R}, P_2)$.

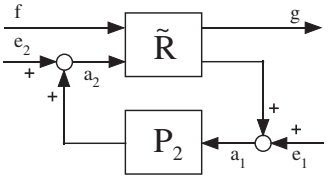

Figure 10. Mapping of $(f'\ e_1'\ e_2')'$ to $(g'\ a_1'\ a_2')'$.

($\Leftarrow$) This way is obvious since internal stability of the system in Figure 9 is equivalent to the transfer function matrix mapping $(f'\ e_1'\ e_2')'$ to $(g'\ a_1'\ a_2')'$ (as shown in Figure 10) being in $\mathscr{RH}_\infty$. Since $F_1(\tilde{R}, P_2)$ maps f to g, $F_1(\tilde{R}, P_2)$ thus belongs to $\mathscr{RH}_\infty$.

($\Rightarrow$) Let P_1 and P_2 have stabilizable and detectable realizations $(A_{P_1}, B_{P_1}, C_{P_1})$ and $(A_{P_2}, B_{P_2}, C_{P_2}, D_{P_2})$, respectively. From the realization for P_1, construct a realization for $\tilde{R}$ as in (6). From Definition A1 in the Appendix, compute the induced realization for $F_1(\tilde{R}, P_2)$ to be

$$\left(\begin{array}{c|c} A_{F_1} & B_{F_1} \\ \hline C_{F_1} & D_{F_1} \end{array}\right)$$

where

$$A_{F_1} := \begin{pmatrix} A_{\tilde{R}} + B_{\tilde{R}_2} D_{P_2} C_{\tilde{R}_2} & B_{\tilde{R}_2} C_{P_2} \\ B_{P_2} C_{\tilde{R}_2} & A_{P_2} \end{pmatrix}$$

$$B_{F_1} := \begin{pmatrix} B_{\tilde{R}_1} + \sqrt{\gamma^2 - 1} B_{\tilde{R}_2} D_{P_2} \\ \sqrt{\gamma^2 - 1} B_{P_2} \end{pmatrix}$$

$$C_{F_1} := (C_{\tilde{R}_1} + D_{P_2} C_{\tilde{R}_2} \quad C_{P_2})$$

$$D_{F_1} := \sqrt{\gamma^2 - 1} D_{P_2}$$

This induced realization is stabilizable and detectable since there exist matrices

$$F_{F_1} = \begin{pmatrix} \dfrac{\gamma}{\sqrt{\gamma^2 - 1}} B_{P_1}^* X & \dfrac{1}{\sqrt{\gamma^2 - 1}} F_{P_2} \end{pmatrix}$$

DOI: 10.1002/rnc

where F_{P_2} is a matrix such that $A_{P_2}+B_{P_2}F_{P_2}$ is Hurwitz and

$$L_{F_1}=\begin{pmatrix}-\gamma\bar{Y}C_{P_1}^{*}\\ L_{P_2}\end{pmatrix}$$

where L_{P_2} is a matrix such that $A_{P_2}+L_{P_2}C_{P_2}$ is Hurwitz such that $A_{F_1}+B_{F_1}F_{F_1}$ and $A_{F_1}+L_{F_1}C_{F_1}$, respectively, are Hurwitz. (Direct substitution shows that $A_{F_1}+L_{F_1}C_{F_1}$ is Hurwitz. Proving that $A_{F_1}+B_{F_1}F_{F_1}$ is Hurwitz is more complicated and the reader is directed to Appendix A.2.) By Theorem A2 in the Appendix, $\bar{n}(F_1(\tilde{R}, P_2))=\bar{n}(V)$, where $V(s)$ denotes the transfer function matrix mapping $(f'\ e_1'\ e_2')'$ to $(g'\ a_1'\ a_2')'$ as shown in Figure 10. If $F_1(\tilde{R}, P_2)\in\mathscr{RH}_\infty$, then $\bar{n}(F_1(\tilde{R}, P_2))=0$ and hence $V\in\mathscr{RH}_\infty$. □

The next result is a consequence of [34, Proposition 1.1]. The result states that stability of a certain transfer function matrix, formed from $\tilde{R}$ and F, is guaranteed.

Lemma 5
Consider a generalized system $F\in\mathscr{R}^{(p+n)\times(q+m)}$ partitioned as in (1), with a stabilizable and detectable realization as given by (2). Suppose that $P_0:=F_{\mathrm{u}}(F, 0)=F_{22}$ has an inherited realization (A, B_2, C_2) from the realization for F, and suppose further that this realization is stabilizable and detectable (see Footnote ‡). Then

$$\tilde{R}\star\begin{pmatrix}P_0 & F_{21}\\ F_{12} & F_{11}\end{pmatrix} \tag{8}$$

belongs to $\mathscr{RH}_\infty$, where $\tilde{R}$ is defined as in (6).

Proof
Note that $\delta_v(P_0, P_0)=0<\beta$; hence, by Cantoni and Vinnicombe [34, Proposition 1.1], $F_1(\tilde{R}, P_0)\in\mathscr{RH}_\infty$. Next, compute the induced realization for $F_1(\tilde{R}, P_0)$ as in Definition A1 of the Appendix, and note that this induced realization is stabilizable and detectable (as was shown for the general case of the induced realization $F_1(\tilde{R}, P_2)$ in the proof of Lemma 4). Since the induced realization for $F_1(\tilde{R}, P_0)$ is stabilizable and detectable, and since $F_1(\tilde{R}, P_0)\in\mathscr{RH}_\infty$, then the '$A$'-matrix of the induced realization for $F_1(\tilde{R}, P_0)$ is Hurwitz. This 'A'-matrix is provided as follows:

$$\begin{pmatrix}A-B_2B_2^{*}X-\gamma^2\bar{Y}C_2^{*}C_2 & \gamma\bar{Y}C_2^{*}C_2\\ -\gamma B_2B_2^{*}X & A\end{pmatrix}$$

where X and Z are the stabilizing solutions to the corresponding generalized algebraic Riccati equations and $\gamma:=1/\beta$, $Y:=(1/(\gamma^2-1))Z$ and $\bar{Y}:=Y(I-XY)^{-1}$. But computation of the induced realization for (8), which is given by

$$\left(\begin{array}{c|cc}A_\star & B_{\star_1} & B_{\star_2}\\ \hline C_{\star_1} & 0 & D_{21}\\ C_{\star_2} & \sqrt{\gamma^2-1}D_{12} & D_{11}\end{array}\right) \tag{9}$$

DOI: 10.1002/rnc

where

$$A_\star := \begin{pmatrix} A - B_2 B_2^* X - \gamma^2 \bar{Y} C_2^* C_2 & \gamma \bar{Y} C_2^* C_2 \\ -\gamma B_2 B_2^* X & A \end{pmatrix}$$

$$B_{\star_1} := \begin{pmatrix} \dfrac{\gamma}{\sqrt{\gamma^2 - 1}} (I - XY)^{-1} B_2 \\ \sqrt{\gamma^2 - 1} B_2 \end{pmatrix}$$

$$B_{\star_2} := \begin{pmatrix} \gamma \bar{Y} C_2^* D_{21} \\ B_1 \end{pmatrix}$$

$$C_{\star_1} := (-\gamma C_2 \;\; C_2)$$

$$C_{\star_2} := (-\gamma D_{12} B_2^* X \;\; C_1)$$

(see [32, Chapter 10.4] for state-space formula), shows that $A_\star$ is equal to the 'A'-matrix of the induced realization for $F_l(\tilde{R}, P_0)$. Hence, (8) is in $\mathscr{RH}_\infty$. □

Remark 6
The induced realization for (8), as given by (9), is stabilizable and detectable since $A_\star$ is Hurwitz.

We are now in the position to show that the LTI quantity on the LHS of (3) can be computed via solving an LMI feasibility problem. Lemmas 4 and 5 are used to obtain an 'upper bound' on the LTI quantity on the LHS of (3), as stated in Theorem 7; then Theorem 7 forms part of the solution algorithm for determining the scaled LTI ν-gap quantity exactly (to within a predetermined tolerance). (This solution algorithm is provided in the following section.) In words, Theorem 7 states the following: given P_0 and F, if a system of LMI constraints dependent on the LTI system $\tilde{R}$ and some given number β is feasible, then the scaled LTI ν-gap quantity on the LHS of (3) is less than or equal to β.

Theorem 7
Suppose that $F \in \mathscr{R}^{(p+n)\times(q+m)}$ is a generalized system partitioned as in (1), with a stabilizable and detectable realization as given by (2); and suppose $P_0 := F_u(F, 0)$ has an inherited realization (A, B_2, C_2) that is also stabilizable and detectable (see Footnote ‡). Consider the LTI uncertainty set $\boldsymbol{\delta_0}$ and the set of constant diagonal matrix pairs $\mathbf{D}$ defined earlier, and suppose that each $\delta \in \boldsymbol{\delta_0}$ has a given stabilizable and detectable realization and that each induced realization for $F_u(F, D_l^{-1} \delta D_r)$ is stabilizable and detectable (as defined in Theorem A2 of the Appendix). Given a $\beta \in (0, b_{\text{opt}}(P_0))$, then

$$\inf_{\widetilde{D}=(D_l, D_r)\in\mathbf{D}} \sup_{\delta\in\boldsymbol{\delta_0}} \delta_\nu(P_0, F_u(F, D_l^{-1}\delta D_r)) \leqslant \beta \tag{10}$$

if $\exists \widetilde{D} \in \mathbf{D} : \forall \omega \in \mathbb{R}\ \exists d_\omega \in \mathbb{R}_+ :$

$$J^*(\mathrm{j}\omega) \begin{pmatrix} d_\omega^2 I_n & 0 \\ 0 & D_r^2 \end{pmatrix} J(\mathrm{j}\omega) < \begin{pmatrix} d_\omega^2 I_m & 0 \\ 0 & D_l^2 \end{pmatrix}$$

DOI: 10.1002/rnc

where

$$J := \tilde{R} \star \begin{pmatrix} P_0 & F_{21} \\ F_{12} & F_{11} \end{pmatrix}$$

and $\tilde{R} \in \mathscr{R}^{(n+m)\times(m+n)}$ is defined as in (6).

Proof
Define

$$H := \begin{pmatrix} 0 & I_n \\ I_p & 0 \end{pmatrix} F \begin{pmatrix} 0 & I_q \\ I_m & 0 \end{pmatrix}$$

so that $J = \tilde{R} \star H$ and $F_{\mathrm{u}}(F, D_{\mathrm{l}}^{-1}\delta D_{\mathrm{r}}) = F_{\mathrm{l}}(H, D_{\mathrm{l}}^{-1}\delta D_{\mathrm{r}})$. Then

$$\begin{aligned} &\inf_{\widetilde{D}=(D_{\mathrm{l}}, D_{\mathrm{r}})\in\mathbf{D}} \sup_{\delta\in\boldsymbol{\delta}_{\mathbf{o}}} \delta_v(P_0, F_{\mathrm{u}}(F, D_{\mathrm{l}}^{-1}\delta D_{\mathrm{r}})) \leqslant \beta \\ &\Leftarrow \exists \widetilde{D} \in \mathbf{D} : \forall \delta \in \boldsymbol{\delta}_{\mathbf{o}} \delta_v(P_0, F_{\mathrm{u}}(F, D_{\mathrm{l}}^{-1}\delta D_{\mathrm{r}})) \leqslant \beta \\ &\Leftrightarrow \exists \widetilde{D} \in \mathbf{D} : \forall \delta \in \boldsymbol{\delta}_{\mathbf{o}} \| F_{\mathrm{l}}(\tilde{R}, F_{\mathrm{l}}(H, D_{\mathrm{l}}^{-1}\delta D_{\mathrm{r}}))\|_\infty \leqslant 1 \text{ and the system in Figure 11 is} \\ &\quad \text{internally stable} \end{aligned} \tag{11}$$

The last equivalence of the above statement is true due to the following. From Lemma 4 we know that

$$\delta_v(P_0, F_{\mathrm{u}}(F, D_{\mathrm{l}}^{-1}\delta D_{\mathrm{r}})) \leqslant \beta$$

$$\Updownarrow$$

$$\| F_{\mathrm{l}}(\tilde{R}, F_{\mathrm{l}}(H, D_{\mathrm{l}}^{-1}\delta D_{\mathrm{r}}))\|_\infty \leqslant 1 \quad \text{and} \quad V \in \mathscr{RH}_\infty$$

where $V(s)$ denotes the transfer function matrix mapping $(f'\ e_1'\ e_2')'$ to $(g'\ a_1'\ a_2')'$ as shown in Figure 12. Now construct a realization for $\tilde{R}$ as in (6); let a stabilizable and detectable realization for a $D_{\mathrm{l}}^{-1}\delta D_{\mathrm{r}}$ be given by $(\breve{A}, \breve{B}, \breve{C}, \breve{D})$ and let an induced realization for an $F_{\mathrm{l}}(H, D_{\mathrm{l}}^{-1}\delta D_{\mathrm{r}})$ (which is stabilizable and detectable due to the supposition in the theorem statement) be given by

$$\left(\begin{array}{c|c} A_{\bar{\eta}} & B_{\bar{\eta}} \\ \hline C_{\bar{\eta}} & D_\eta \end{array}\right)$$

where

$$A_{\bar{\eta}} := \begin{pmatrix} 0 & I \\ I & 0 \end{pmatrix} A_\eta \begin{pmatrix} 0 & I \\ I & 0 \end{pmatrix}, \quad B_{\bar{\eta}} := \begin{pmatrix} 0 & I \\ I & 0 \end{pmatrix} B_\eta, \quad C_{\bar{\eta}} := C_\eta \begin{pmatrix} 0 & I \\ I & 0 \end{pmatrix}$$

and A_η, B_η, C_η are given in Definition A1 of the Appendix. Then $V \in \mathscr{RH}_\infty$ if and only if the 'A'-matrix of the induced realization for $V(s)$, given by

$$\left(\begin{array}{c|c} A_V & B_V \\ \hline C_V & D_V \end{array}\right)$$

DOI: 10.1002/rnc

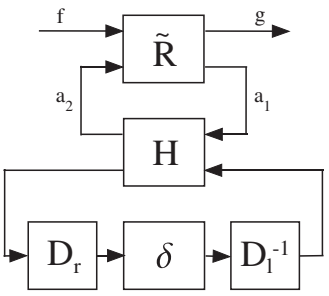

Figure 11. Internal stability of $F_l(J, D_l^{-1}\delta D_r)$.

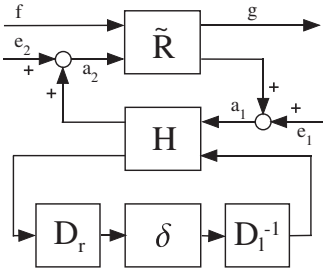

Figure 12. Mapping of $(f'\ e_1'\ e_2')'$ to $(g'\ a_1'\ a_2')'$.

where

$$A_V := \begin{pmatrix} A_{\tilde{R}} + B_{\tilde{R}_2} D_\eta C_{\tilde{R}_2} & B_{\tilde{R}_2} C_{\bar{\eta}} \\ B_{\bar{\eta}} C_{\tilde{R}_2} & A_{\bar{\eta}} \end{pmatrix}$$

$$B_V := \begin{pmatrix} B_{\tilde{R}_1} + \sqrt{\gamma^2 - 1} B_{\tilde{R}_2} D_\eta & B_{\tilde{R}_2} D_\eta & B_{\tilde{R}_2} \\ \sqrt{\gamma^2 - 1} B_{\bar{\eta}} & B_{\bar{\eta}} & 0 \end{pmatrix}$$

$$C_V := \begin{pmatrix} C_{\tilde{R}_1} + D_\eta C_{\tilde{R}_2} & C_{\bar{\eta}} \\ C_{\tilde{R}_2} & 0 \\ D_\eta C_{\tilde{R}_2} & C_{\bar{\eta}} \end{pmatrix}$$

$$D_V := \begin{pmatrix} \sqrt{\gamma^2 - 1} D_\eta & D_\eta & I \\ \sqrt{\gamma^2 - 1} I & I & 0 \\ \sqrt{\gamma^2 - 1} D_\eta & D_\eta & I \end{pmatrix}$$

is Hurwitz [33, Lemma A.4.1].

DOI: 10.1002/rnc

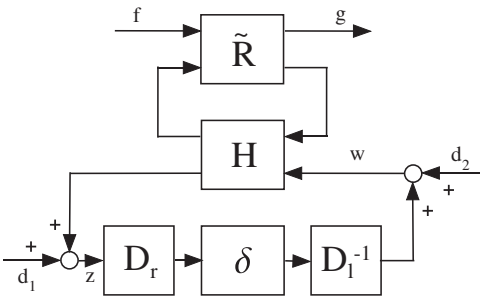

Figure 13. Mapping of $(f'\ d_1'\ d_2')'$ to $(g'\ z'\ w')'$.

Now construct the induced realization for J as in (9), noting that stabilizability and detectability of this realization is guaranteed (see Remark 6). Let $\bar{U}(s)$ denote the transfer function matrix mapping $(f'\ d_1'\ d_2')'$ to $(g'\ z'\ w')'$ as shown in Figure 13. It is true that $\bar{U} \in \mathscr{RH}_\infty$ if and only if the 'A'-matrix of the induced realization for $\bar{U}(s)$, given by

$$\left(\begin{array}{c|c} A_{\bar{U}} & B_{\bar{U}} \\ \hline C_{\bar{U}} & D_{\bar{U}} \end{array}\right)$$

where

$$A_{\bar{U}} := \begin{pmatrix} A_\star + B_{\star_2} Q \breve{D} C_{\star_2} & B_{\star_2} Q \breve{C} \\ \breve{B} R C_{\star_2} & \breve{A} + \breve{B} R D_{11} \breve{C} \end{pmatrix}$$

$$B_{\bar{U}} := \begin{pmatrix} B_{\star_1} + \sqrt{\gamma^2 - 1} B_{\star_2} Q \breve{D} D_{12} & B_{\star_2} Q \breve{D} & B_{\star_2} Q \\ \sqrt{\gamma^2 - 1} \breve{B} R D_{12} & \breve{B} R & \breve{B} R D_{11} \end{pmatrix}$$

$$C_{\bar{U}} := \begin{pmatrix} C_{\star_1} + D_{21} Q \breve{D} C_{\star_2} & D_{21} Q \breve{C} \\ R C_{\star_2} & R D_{11} \breve{C} \\ Q \breve{D} C_{\star_2} & Q \breve{C} \end{pmatrix}$$

$$D_{\bar{U}} := \begin{pmatrix} \sqrt{\gamma^2 - 1} D_{21} Q \breve{D} D_{12} & D_{21} Q \breve{D} & D_{21} Q \\ \sqrt{\gamma^2 - 1} R D_{12} & R & R D_{11} \\ \sqrt{\gamma^2 - 1} Q \breve{D} D_{12} & Q \breve{D} & Q \end{pmatrix}$$

$R := (I - D_{11}\breve{D})^{-1}$ and $Q := (I - \breve{D} D_{11})^{-1}$, is Hurwitz. A simple calculation shows that $A_V = A_{\bar{U}}$.

Note that

$$F_l(\tilde{R}, F_l(H, D_l^{-1} \delta D_r)) = F_l(J, D_l^{-1} \delta D_r) = F_u(G, \delta)$$

DOI: 10.1002/rnc

where

$$G := \begin{pmatrix} 0 & D_{\mathrm{r}} \\ I_n & 0 \end{pmatrix} J \begin{pmatrix} 0 & I_m \\ D_{\mathrm{l}}^{-1} & 0 \end{pmatrix}$$

This means that (11) holds

$$\begin{aligned} &\Leftrightarrow \exists \widetilde{D} \in \mathbf{D} : \forall \delta \in \boldsymbol{\delta}_{\mathbf{o}} \| F_{\mathrm{u}}(G, \delta) \|_\infty \leqslant 1 \text{ and the system in Figure 11 is internally stable} \\ &\Leftrightarrow \exists \widetilde{D} \in \mathbf{D} : \sup_{\omega \in \mathbb{R}} \mu_{\boldsymbol{\delta}_{\mathbf{s}}}(G(\mathrm{j}\omega)) \leqslant 1 \end{aligned} \tag{12}$$

where μ is the structured singular value with respect to the structured set

$$\boldsymbol{\delta}_{\mathbf{s}} := \left\{ \begin{pmatrix} \delta & 0 \\ 0 & \hat{\delta} \end{pmatrix} : \hat{\delta} \in \mathscr{RH}_\infty^{m \times n}, \| \hat{\delta} \|_\infty < 1, \delta \in \boldsymbol{\delta}_{\mathbf{o}} \right\}$$

using [32, Theorem 11.9] and noting that $J \in \mathscr{RH}_\infty$ from Lemma 5. Finally, let $d_\omega \in \mathbb{R}_+$ such that

$$\begin{pmatrix} I_q & 0 \\ 0 & d_\omega I_m \end{pmatrix} \begin{pmatrix} \delta & 0 \\ 0 & \hat{\delta} \end{pmatrix} \begin{pmatrix} I_p & 0 \\ 0 & \dfrac{1}{d_\omega} I_n \end{pmatrix} = \begin{pmatrix} \delta & 0 \\ 0 & \hat{\delta} \end{pmatrix}$$

for all

$$\begin{pmatrix} \delta & 0 \\ 0 & \hat{\delta} \end{pmatrix} \in \boldsymbol{\delta}_{\mathbf{s}}$$

At each frequency ω, $\mu_{\boldsymbol{\delta}_{\mathbf{s}}}(G(\mathrm{j}\omega))$ is equal to

$$\inf_{d_\omega \in \mathbb{R}_+} \bar{\sigma} \left(\begin{pmatrix} 0 & D_{\mathrm{r}} \\ d_\omega I_n & 0 \end{pmatrix} J(\mathrm{j}\omega) \begin{pmatrix} 0 & \dfrac{1}{d_\omega} I_m \\ D_{\mathrm{l}}^{-1} & 0 \end{pmatrix} \right)$$

from [32, Theorem 11.5], where $\bar{\sigma}$ denotes the maximum singular value. Therefore, (12) holds

$$\begin{aligned} &\Leftarrow \exists \widetilde{D} \in \mathbf{D} : \forall \omega \in \mathbb{R}\ \exists d_\omega \in \mathbb{R}_+ : \bar{\sigma} \left(\begin{pmatrix} 0 & D_{\mathrm{r}} \\ d_\omega I_n & 0 \end{pmatrix} J(\mathrm{j}\omega) \begin{pmatrix} 0 & \dfrac{1}{d_\omega} I_m \\ D_{\mathrm{l}}^{-1} & 0 \end{pmatrix} \right) \leqslant 1 \\ &\Leftrightarrow \exists \widetilde{D} \in \mathbf{D} : \forall \omega \in \mathbb{R}\ \exists d_\omega \in \mathbb{R}_+ : J^*(\mathrm{j}\omega) \begin{pmatrix} d_\omega^2 I_n & 0 \\ 0 & D_{\mathrm{r}}^2 \end{pmatrix} J(\mathrm{j}\omega) \leqslant \begin{pmatrix} d_\omega^2 I_m & 0 \\ 0 & D_{\mathrm{l}}^2 \end{pmatrix} \end{aligned} \qquad \square$$

The implications that are not necessary and sufficient in the above proof could be easily tightened to necessary and sufficient implications by replacing several $\leqslant$ with $<$ and considering the closed set $\boldsymbol{\delta}$ and $\mathbb{R} \cup \{\infty\}$ where appropriate, similar to the proof of Theorem 3. However, one key equivalence in the above proof relating a ν-gap ball to a $\mathscr{H}_\infty$-ball (see Lemma 4 based on [34, Proposition 1.1]) is only stated in terms of non-strict inequalities. It may or may not be possible

DOI: 10.1002/rnc

to rewrite Lemma 4 with strict inequalities, thereby allowing for a tightening of Theorem 7 so that it is necessary and sufficient; this has not been investigated in this paper. At this stage, we simply point out that the condition in Theorem 7, as expressed, is 'close to' necessary for (10) to hold, as necessity is only lost at closure of sets $\boldsymbol{\delta}_{\mathbf{0}}, \mathbb{R}, \mathbf{D}$.

5. SOLUTION ALGORITHM

A solution algorithm that can be used to determine the exact scaled LTI quantity on the LHS of (3) is now provided. The solution algorithm itself is based on a standard bisectional search. The notion is to use Theorem 7 to determine feasibility of a system of LMI constraints with respect to a test value β. Iterations of the bisectional line search are implemented over the interval $(0, b_{\mathrm{opt}}(P_0))$ to select subsequent test values for β. The direction in which the line search proceeds depends on the 'true' or 'false' result acquired by solving the LMI feasibility problem: a 'false' result suggests that a larger test β should be chosen; whereas a 'true' result indicates that one can try a smaller test β. Consequently, the LTI quantity $\inf_{\widetilde{D}=(D_{\mathrm{l}}, D_{\mathrm{r}})\in\mathbf{D}} \sup_{\delta\in\boldsymbol{\delta}_{\mathbf{0}}} \delta_v(P_0, F_{\mathrm{u}}(F, D_{\mathrm{l}}^{-1}\delta D_{\mathrm{r}}))$ is achieved to within a sufficiently small pre-determined tolerance. Provided that the LTI quantity obtained is smaller than the generalized robust stability margin $b_{P_0,K}$ achieved with some controller K that internally stabilizes the nominal plant, then internal stability of the system $[P_{\mathrm{LTV}}, K]$ for all time-varying perturbations $\Delta\in\boldsymbol{\Delta}$ is guaranteed.

The complete solution algorithm is as follows:

(1) Set the bounds on possible β to be $\alpha_{\mathrm{l}}=0$ and $\alpha_{\mathrm{r}}=b_{\mathrm{opt}}(P_0)$. Set a sufficiently small tolerance $\varepsilon>0$ for the iterative bisections with respect to finding β to end. Select an initial $\beta_0=\alpha_{\mathrm{r}}-\varepsilon$ and set $\beta_{\mathrm{feas}}=b_{\mathrm{opt}}(P_0)$. Set $i=0$. Go to Step 2.

(2) Given a β_i, solve the convex optimization problem: 'does there exist a $\widetilde{D}\in\mathbf{D}$ such that, for each $\omega\in\mathbb{R}$, there exists a corresponding $d_\omega\in\mathbb{R}_+$ such that

$$J^*(\mathrm{j}\omega)\begin{pmatrix} d_\omega^2 I_n & 0 \\ 0 & D_{\mathrm{r}}^2 \end{pmatrix} J(\mathrm{j}\omega) \leqslant \begin{pmatrix} d_\omega^2 I_m & 0 \\ 0 & D_{\mathrm{l}}^2 \end{pmatrix}$$

where

$$J := \tilde{R}\star\begin{pmatrix} P_0 & F_{21} \\ F_{12} & F_{11} \end{pmatrix}$$

and $\tilde{R}$ is defined as in (6)'. Now,

(i) If the optimization problem is feasible, set $\beta_{\mathrm{feas}}=\beta_i$ and $\beta_{i+1}=(\alpha_{\mathrm{l}}+\beta_i)/2$. Update $\alpha_{\mathrm{r}}=\beta_i$. Go to Step 2(iii).

(ii) If the optimization problem is not feasible, test whether $\beta_{\mathrm{feas}}-\beta_i\leqslant\varepsilon$. If yes, then end. If no, set $\beta_{i+1}=(\beta_i+\alpha_{\mathrm{r}})/2$. Update $\alpha_{\mathrm{l}}=\beta_i$. Go to Step 2(iii).

(iii) Set $i=i+1$ and go to Step 2.

If $\beta_{\mathrm{feas}}<b_{P_0,K}$, where K is some internally stabilizing controller, then $[P_{\mathrm{LTV}}, K]$ is internally stable for all $\Delta\in\boldsymbol{\Delta}$. If not, internal stability of $[P_{\mathrm{LTV}}, K]$ has not been determined (and a possibility if $\beta_{\mathrm{feas}}\neq b_{\mathrm{opt}}(P_0)$ is to choose a different controller to obtain a larger stability margin).

DOI: 10.1002/rnc

The convex optimization problem in Step 2 of the solution algorithm is easily solved using Matlab's LMI toolbox, for instance. A numerical example follows in the following section for completeness.

6. NUMERICAL EXAMPLE

The following example illustrates the implementation of the solution algorithm. The example has been taken from [38]. In [38], an optimization problem that integrates a number of steps of the standard $\mathscr{H}_\infty$ loop-shaping design procedure [39] is introduced. The idea is to maximize the generalized robust stability margin of the shaped plant $P_s = W_2 P W_1$, where P is the scaled nominal open-loop plant, over allowable loop-shaping weights W_1 and W_2, while ensuring that the resulting loop shape lies in a pre-defined region that characterizes the desired performance specifications (see Figure 14).

The plant used in the example in [38] is a scaled-down version of the high incidence research model developed by the Defence Evaluation and Research Agency in Bedford, U.K. A physical model of this was constructed at the University of Cambridge in order to investigate problems associated with the control of air vehicles at high angles of attack. Details of the experiment carried out on this plant may be found in [40].

Input data for the following was given in [38, Section 5]: the scaled nominal open-loop plant P; the loop-shape boundaries; and the loop-shape weight singular value and condition number bounds. Implementation of the algorithm presented in [38] (for the case in which a diagonal pre-compensator W_1 is required and the post-compensator W_2 is held fixed) produced the maximized value of $b_{\text{opt}}(P_s)$, the loop-shaping weights W_1 and W_2 that achieved this maximized robust stability margin, and a robustly (in terms of stable LTI perturbations to the coprime factors of P_s) stabilizing controller K_∞ as output. In particular, the shaped plant $P_s = W_2 P W_1$ was found to be given by the state-space model shown in Figure 15, and $b_{\text{opt}}(P_s)$ was found to be 0.376 using Matlab's μ-Analysis and Synthesis Toolbox 'ncfsyn' function.

Suppose a control system designer wanted to determine to what extent the feedback interconnection shown in Figure 14 would remain internally stable in the face of LTV uncertainty. For instance, consider the uncertain-shaped plant shown in Figure 16, where Δ_1 and Δ_2 represent output multiplicative and input feedback LTV uncertainties, respectively. Formally, the uncertain-shaped plant model shown in Figure 16 is described by

$$(I + \varepsilon_1 \Delta_1) P_s (I - \varepsilon_2 \Delta_2)^{-1} \tag{13}$$

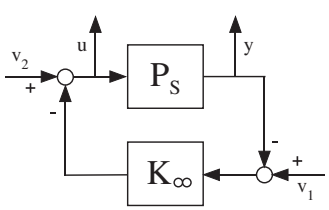

Figure 14. $\mathscr{H}_\infty$ loop-shaping framework.

DOI: 10.1002/rnc

$$\left(\begin{array}{cccccccccccccccc|cc}
0 & 1.00 & 0 & 0 & 0 & 0 & 0 & 0 & 0 & 0 & 0 & 0 & 0 & 0 & 0 & 0 & 0 & 0 \\
-23.8 & -3.36 & 4.60 & -0.239 & 11.8 & 0 & 0 & 0 & 0 & 0 & 0 & 0 & 0 & 0 & 0 & 0 & 0 & 0 \\
0 & 0 & 0 & 1.00 & 0 & 0 & 0 & 0 & 0 & 0 & 0 & 0 & 0 & 0 & 0 & 0 & 0 & 0 \\
-16.8 & -0.0248 & 22.8 & -0.916 & 0 & 0 & 9.83 & 0 & 0 & 0 & 0 & 0 & 0 & 0 & 0 & 0 & 0 & 0 \\
0 & 0 & 0 & 0 & -50.0 & 63.2 & 0 & 0 & 112 & -9590 & -1530 & -1250 & 0 & 0 & 0 & 0 & -45300 & 0 \\
0 & 0 & 0 & 0 & 0 & -40.0 & 0 & 0 & -142 & 12100 & 1930 & 1580 & 0 & 0 & 0 & 0 & 57400 & 0 \\
0 & 0 & 0 & 0 & 0 & 0 & -50.0 & 63.2 & 0 & 0 & 0 & 0 & -58.0 & 10600 & -145 & -1320 & 0 & -55500 \\
0 & 0 & 0 & 0 & 0 & 0 & 0 & -40.0 & 0 & 0 & 0 & 0 & 73.3 & -13400 & 183 & 1670 & 0 & 70200 \\
0 & 0 & 0 & 0 & 0 & 0 & 0 & 0 & -0.00561 & 1.14 & 0.178 & 0.123 & 0 & 0 & 0 & 0 & -15.9 & 0 \\
0 & 0 & 0 & 0 & 0 & 0 & 0 & 0 & -1.14 & -258 & -43.9 & -74.7 & 0 & 0 & 0 & 0 & -1360 & 0 \\
0 & 0 & 0 & 0 & 0 & 0 & 0 & 0 & -0.178 & -43.9 & -7.52 & -13.9 & 0 & 0 & 0 & 0 & -216 & 0 \\
0 & 0 & 0 & 0 & 0 & 0 & 0 & 0 & 0.123 & 74.7 & 13.9 & -43.9 & 0 & 0 & 0 & 0 & 177 & 0 \\
0 & 0 & 0 & 0 & 0 & 0 & 0 & 0 & 0 & 0 & 0 & 0 & -0.00271 & 1.52 & -0.0158 & -0.120 & 0 & 8.20 \\
0 & 0 & 0 & 0 & 0 & 0 & 0 & 0 & 0 & 0 & 0 & 0 & -1.52 & -262 & 5.05 & 72.0 & 0 & 1500 \\
0 & 0 & 0 & 0 & 0 & 0 & 0 & 0 & 0 & 0 & 0 & 0 & 0.0158 & 5.05 & -0.117 & -2.76 & 0 & -20.5 \\
0 & 0 & 0 & 0 & 0 & 0 & 0 & 0 & 0 & 0 & 0 & 0 & -0.120 & -72.0 & 2.76 & -43.9 & 0 & 187 \\
\hline
1 & 0 & 0 & 0 & 0 & 0 & 0 & 0 & 0 & 0 & 0 & 0 & 0 & 0 & 0 & 0 & 0 & 0 \\
0 & 0 & 1 & 0 & 0 & 0 & 0 & 0 & 0 & 0 & 0 & 0 & 0 & 0 & 0 & 0 & 0 & 0
\end{array}\right)$$

Figure 15. State-space model of P_s.

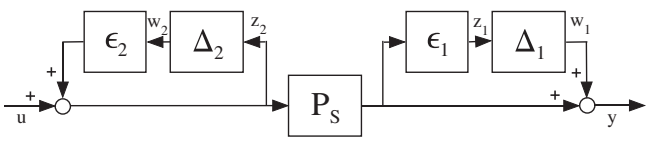

Figure 16. Open-loop shaped plant with uncertainty.

where $\Delta_1, \Delta_2 \in \mathbf{\Delta}$, and $\varepsilon_1, \varepsilon_2 \in [0, 1]$. Recall that output multiplicative uncertainty may typically represent output (sensor) errors or neglected high-frequency dynamics, whereas input feedback uncertainty may represent low-frequency parameter errors (see [32, Table 9.1]). Expressing (13) in the standard structured uncertainty form gives

$$F = \begin{pmatrix} 0 & \varepsilon_1 \varepsilon_2 P_s & \varepsilon_1 P_s \\ 0 & \varepsilon_2 I & I \\ I & \varepsilon_2 P_s & P_s \end{pmatrix}$$

(and so F is a transfer function matrix that relates the structure of the uncertainties Δ_1 and Δ_2 to P_s).

The solution algorithm presented in this paper can be, and was, used to determine stability robustness of the uncertain feedback interconnection. The input to the algorithm consisted of the state-space model of the shaped plant P_s as given in Figure 15, a (stabilizable and detectable) state-space model for the transfer function matrix F such that the state-space model for P_s was inherited from F and the realizations for F_{21} and F_{12} had no unstable invariant zeros, and the size of the scaling factors ε_1 and ε_2. The algorithm was coded up in Matlab 6.5. One hundred equally spaced frequency points on a logarithmic scale between $\omega = 10^{-4}$ and 10^4 rad/s were chosen for Step 2 of the algorithm and a tolerance of 0.001 was chosen for Step 1.

First, stability robustness of the system subject only to output multiplicative uncertainty was investigated. Four hundred and one evenly spaced scaling factors ε_1 were chosen from between $[0, 1]$ to represent different sizes of the uncertainty, whereas ε_2 was set fixed at zero. An algorithm output quantity β_{feas} (representative of the LTI quantity on the LHS of (3)) was produced for each of the 401 pairs of uncertainty scaling factors $(\varepsilon_1, \varepsilon_2)$. The results for which $\varepsilon_1 \in [0, 0.5]$ are shown in Figure 17. For example, a size of $\varepsilon_1 = 0.4975$ resulted in a β_{feas} of 0.367, which

DOI: 10.1002/rnc

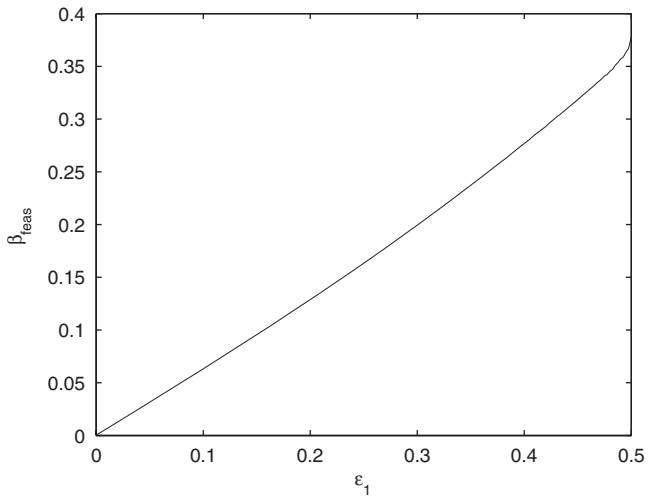

Figure 17. The quantity β_{feas} with respect to the size of the output multiplicative uncertainty.

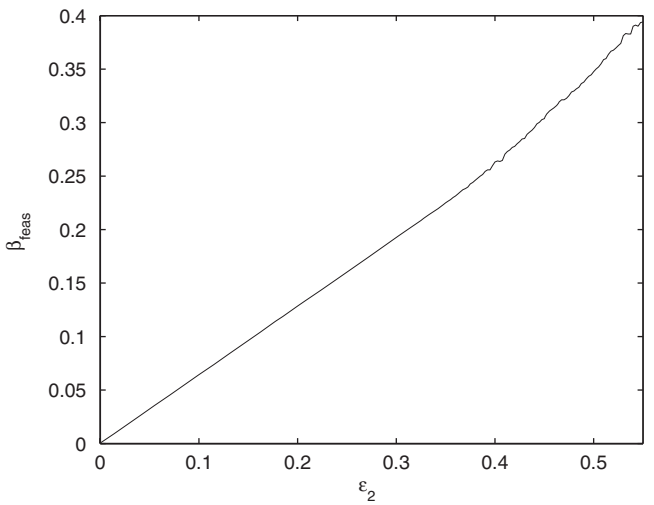

Figure 18. The quantity β_{feas} with respect to the size of the input feedback uncertainty.

is less than $b_{\text{opt}}(P_{\text{s}})=0.376$. This means that the interconnection $[P_{\text{s}}, K_{\infty}]$ subject to LTV output multiplicative uncertainties with scaling factors of size up to and including 0.4975 as described by (13), will be internally stable. Note that the next (larger) scaling factor tested was $\varepsilon_1=0.5$, for which the algorithm produced an output $\beta_{\text{feas}}>b_{\text{opt}}(P_{\text{s}})$ and so internal stability of $[P_{\text{s}}, K_{\infty}]$ subject to LTV output multiplicative uncertainties with $\varepsilon_1>0.4975$ was not concluded here.

Next, stability robustness of the system subject only to input feedback uncertainty was investigated. The scaling factor ε_1 was set fixed at zero and β_{feas} was computed with respect to 401 evenly spaced input feedback uncertainty scaling factors ε_2 ranging from between $[0, 1]$. The results for

DOI: 10.1002/rnc

which ε_2 ranged between $[0, 0.55]$ are shown in Figure 18. Here, a size of $\varepsilon_2 = 0.5275$ resulted in an LTI quantity of 0.374, which is less than $b_{\text{opt}}(P_s)$, and so $[P_s, K_\infty]$ subject to LTV input feedback uncertainties of size less than or equal to 0.5275 as described by (13) was guaranteed to be internally stable. Again, internal stability when $\varepsilon_2 > 0.5275$ could not be concluded.

Finally, stability robustness of the feedback interconnection was tested with respect to when P_s was subjected to both output multiplicative and input feedback LTV uncertainties. For example, when the scaling factors were set to $\varepsilon_1 = 0.35$ and $\varepsilon_2 = 0.38$, the algorithm produced a β_{feas} of 0.371, meaning that $[P_s, K_\infty]$ subject to both output multiplicative and input feedback LTV uncertainties of sizes 0.35 and 0.38, respectively, as described by (13), is guaranteed to be internally stable.

7. CONCLUSIONS AND FUTURE WORK

The scaled small gain condition, traditionally used to determine stability robustness of LTI nominal systems subject to structured LTV uncertainty, was utilized to formulate a stability robustness condition for the same problem in a scaled LTI ν-gap metric framework. It was shown that the scaled LTI ν-gap metric condition can be checked via solving an LMI feasibility problem (as can the scaled small gain condition). A key difference between the scaled small gain condition and the condition presented in this paper is that the LMI feasibility problem associated with the scaled LTI ν-gap metric condition is independent of knowledge about the controller. Thus, the scaled LTI ν-gap metric condition provides a single constraint on a controller (in terms of a large enough generalized robust stability margin) that (sufficiently) guarantees to stabilize all plants in the uncertainty set. Further investigation into the conservatism of the test is now required.

APPENDIX A

A.1. Induced realizations for LFTS

In this section, the induced realization for an upper or lower LFT is formally defined. We also present a result concerning stabilizability and detectability of induced realizations.

Let a stabilizable and detectable realization** for a generalized system $F \in \mathscr{R}^{(p+n)\times(q+m)}$ be given by

$$\left(\begin{array}{c|cc} A & B_1 & B_2 \\ \hline C_1 & D_{11} & D_{12} \\ C_2 & D_{21} & 0 \end{array}\right) \tag{A1}$$

and let stabilizable and detectable realizations for a controller $K \in \mathscr{R}^{m\times n}$ and an uncertain system $E \in \mathscr{R}^{q\times p}$ be given by $(\hat{A}, \hat{B}, \hat{C}, \hat{D})$ and $(\breve{A}, \breve{B}, \breve{C}, \breve{D})$, respectively. Note that a realization (A, B, C, D) for a transfer function matrix $X(s)$ is stabilizable and detectable if and only if $\bar{n}(X) = \bar{\lambda}(A)$, where $\bar{n}(\cdot)$ denotes the number of closed RHP poles counted according to the usual notion of the Smith–McMillan decomposition, and $\bar{\lambda}(\cdot)$ denotes the number of eigenvalues with real part in the closed RHP. This result is a consequence of the fact that the only uncontrollable

**The D_{22} term has been absorbed into the controller by a loop-shifting argument (see [33, Section 4.6], for instance).

DOI: 10.1002/rnc

and unobservable modes in (A, B, C, D) must be in $Re(s)<0$ if the realization is stabilizable and detectable.

Definition A1
The induced realization for[††]

(a) $F_l(F, K)$ is the realization formed from the above-stated realizations for $F \in \mathscr{R}^{(p+n)\times(q+m)}$ and $K \in \mathscr{R}^{m\times n}$ as given by

$$\left(\begin{array}{c|c} A_\theta & B_\theta \\ \hline C_\theta & D_\theta \end{array}\right)$$

where

$$A_\theta := \begin{pmatrix} A + B_2\hat{D}C_2 & B_2\hat{C} \\ \hat{B}C_2 & \hat{A} \end{pmatrix}$$

$$B_\theta := \begin{pmatrix} B_1 + B_2\hat{D}D_{21} \\ \hat{B}D_{21} \end{pmatrix}$$

$$C_\theta := (C_1 + D_{12}\hat{D}C_2 \quad D_{12}\hat{C})$$

$$D_\theta := D_{11} + D_{12}\hat{D}D_{21}$$

(b) $F_u(F, E)$ is the realization formed from the above-stated realizations for $F \in \mathscr{R}^{(p+n)\times(q+m)}$ and $E \in \mathscr{R}^{q\times p}$ as given by

$$\left(\begin{array}{c|c} A_\eta & B_\eta \\ \hline C_\eta & D_\eta \end{array}\right) \tag{A2}$$

where

$$A_\eta := \begin{pmatrix} \breve{A} + \breve{B}RD_{11}\breve{C} & \breve{B}RC_1 \\ B_1Q\breve{C} & A + B_1Q\breve{D}C_1 \end{pmatrix}$$

$$B_\eta := \begin{pmatrix} \breve{B}RD_{12} \\ B_1Q\breve{D}D_{12} + B_2 \end{pmatrix}$$

$$C_\eta := (D_{21}Q\breve{C} \quad D_{21}Q\breve{D}C_1 + C_2)$$

$$D_\eta := D_{21}Q\breve{D}D_{12}$$

and $R := (I - D_{11}\breve{D})^{-1}$, $Q := (I - \breve{D}D_{11})^{-1}$.

[††]The induced realization is also referred to as the *natural realization* in the literature (see [33, Lemma 4.1.2], for instance).

DOI: 10.1002/rnc

Stabilizability and detectability of the induced realization for $F_u(F, E)$ is considered in the following result.

Theorem A2
Consider a generalized plant $F \in \mathscr{R}^{(p+n)\times(q+m)}$ and an LTI uncertainty $E \in \mathscr{R}^{q\times p}$. Suppose that a stabilizable and detectable realization for F is given by (A1) and that E has a given stabilizable and detectable realization. Then the induced realization for $F_u(F, E)$, defined as in Definition A1, is stabilizable and detectable if and only if $\bar{n}(F_u(F, E)) = \bar{n}(T)$, where $\bar{n}(\cdot)$ denotes the number of closed RHP poles counted according to the usual notion of the Smith–McMillan decomposition, and $T(s)$ denotes the transfer function matrix mapping $(d_2' \; d_1' \; u')'$ to $(w' \; z' \; y')'$ as shown in Figure A1.

In addition, the induced realization for $F_u(F, E)$ is

(a) detectable if

$$\begin{pmatrix} A-\lambda I & B_1 \\ C_2 & D_{21} \end{pmatrix}$$

has full column rank $\forall Re(\lambda) \geqslant 0$;

(b) stabilizable if

$$\begin{pmatrix} A-\lambda I & B_2 \\ C_1 & D_{12} \end{pmatrix}$$

has full row rank $\forall Re(\lambda) \geqslant 0$.

Proof
Parts (a) and (b) of the final part of Theorem A2 are from [32, Lemma 16.1], with their proof supplied in that reference. It remains to prove the necessary and sufficient condition for stabilizability and detectability of the induced realization.

Let the stabilizable and detectable realization for E be given by $(\breve{A}, \breve{B}, \breve{C}, \breve{D})$. The induced realization for $T(s)$ is given by

$$\left(\begin{array}{c|c} A_T & B_T \\ \hline C_T & D_T \end{array}\right) \tag{A3}$$

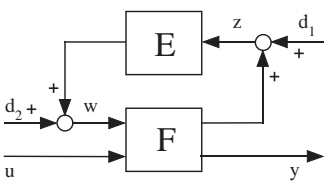

Figure A1. Mapping of $(d_2' \; d_1' \; u')'$ to $(w' \; z' \; y')'$.

DOI: 10.1002/rnc

where

$$A_T := \begin{pmatrix} \breve{A}+\breve{B}RD_{11}\breve{C} & \breve{B}RC_1 \\ B_1Q\breve{C} & A+B_1Q\breve{D}C_1 \end{pmatrix}$$

$$B_T := \begin{pmatrix} \breve{B}RD_{11} & \breve{B}R & \breve{B}RD_{12} \\ B_1Q & B_1Q\breve{D} & B_1Q\breve{D}D_{12}+B_2 \end{pmatrix}$$

$$C_T := \begin{pmatrix} Q\breve{C} & Q\breve{D}C_1 \\ RD_{11}\breve{C} & RC_1 \\ D_{21}Q\breve{C} & D_{21}Q\breve{D}C_1+C_2 \end{pmatrix}$$

$$D_T := \begin{pmatrix} Q & Q\breve{D} & Q\breve{D}D_{12} \\ RD_{11} & R & RD_{12} \\ D_{21}Q & D_{21}Q\breve{D} & D_{21}Q\breve{D}D_{12} \end{pmatrix}$$

and $R := (I - D_{11}\breve{D})^{-1}$, $Q := (I - \breve{D}D_{11})^{-1}$. This induced realization is stabilizable and detectable. To see detectability, suppose that

$$\begin{pmatrix} \breve{A}+\breve{B}RD_{11}\breve{C}-\lambda I & \breve{B}RC_1 \\ B_1Q\breve{C} & A+B_1Q\breve{D}C_1-\lambda I \\ Q\breve{C} & Q\breve{D}C_1 \\ RD_{11}\breve{C} & RC_1 \\ D_{21}Q\breve{C} & D_{21}Q\breve{D}C_1+C_2 \end{pmatrix} \times \begin{pmatrix} w_1 \\ w_2 \end{pmatrix} = \begin{pmatrix} 0 \\ 0 \\ 0 \\ 0 \\ 0 \end{pmatrix}$$

Then, row 3 and row $4 \Rightarrow C_1 w_2 = 0$ and $\breve{C} w_1 = 0$, row $5 \Rightarrow C_2 w_2 = 0$, row $1 \Rightarrow (\breve{A} - \lambda I) w_1 = 0$, and row $2 \Rightarrow (A - \lambda I) w_2 = 0$. Since

$$\left(\begin{pmatrix} C_1 \\ C_2 \end{pmatrix}, A \right)$$

and $(\breve{C}, \breve{A})$ are detectable, $w_1 = 0$ and $w_2 = 0$ for all $Re(\lambda) \geqslant 0$ and hence (A3) is detectable. Stabilizability of (A3) may be similarly established. Therefore, $\bar{n}(T) = \bar{\lambda}(A_T)$.

However, from the observation of (A2), $A_T = A_\eta$. Consequently, it must be shown that (A2) is stabilizable and detectable if and only if $\bar{n}(F_u(F, E)) = \bar{\lambda}(A_\eta)$. If (A2) is stabilizable and detectable, then $\bar{n}(F_u(F, E)) = \bar{\lambda}(A_\eta)$. If (A2) is not stabilizable and/or not detectable, then A_η has an unstable hidden mode, which implies that $\bar{n}(F_u(F, E)) < \bar{\lambda}(A_\eta)$. □

Parts (a) and (b) of the final part of Theorem A2 have been given because the necessary and sufficient condition stated in the earlier part of the theorem is dependent on E, and can hence be

DOI: 10.1002/rnc

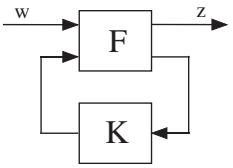

Figure A2. System representation of $F_l(F, K)$.

difficult to check. This is as opposed to the sufficient conditions in (a) and (b), which are equivalent to requiring no unstable invariant zeros of the realizations

$$\left(\begin{array}{c|c} A & B_1 \\ \hline C_2 & D_{21} \end{array}\right) \quad \text{and} \quad \left(\begin{array}{c|c} A & B_2 \\ \hline C_1 & D_{12} \end{array}\right)$$

for F_{21} and F_{12}, respectively.

Now suppose that $P_0 := F_u(F, 0) = F_{22}$ has a realization (A, B_2, C_2) which is inherited from (A1), and suppose further that this realization is stabilizable and detectable (see Footnote ‡). Then suppose that K has a stabilizable and detectable realization $(\hat{A}, \hat{B}, \hat{C}, \hat{D})$, and that $[P_0, K]$ as shown in Figure 1 is internally stable. An immediate consequence is stabilizability and detectability of the induced realization for $F_l(F, K)$. To see this, suppose that x and $\hat{x}$ denote the state vectors for the realizations for P_0 and K, respectively, the state equations corresponding to Figure 1 with $v_1 = v_2 = 0$ are

$$\dot{x} = Ax + B_2 u \tag{A4}$$

$$y = C_2 x \tag{A5}$$

$$\dot{\hat{x}} = \hat{A}\hat{x} + \hat{B}y \tag{A6}$$

$$u = \hat{C}\hat{x} + \hat{D}y \tag{A7}$$

Solving (A5) and (A7) for u and y, and substituting into (A4) and (A6) gives

$$\begin{pmatrix} \dot{x} \\ \dot{\hat{x}} \end{pmatrix} = \tilde{A} \begin{pmatrix} x \\ \hat{x} \end{pmatrix}$$

where

$$\tilde{A} := \begin{pmatrix} A + B_2 \hat{D} C_2 & B_2 \hat{C} \\ \hat{B} C_2 & \hat{A} \end{pmatrix}$$

is Hurwitz [32, Lemma 5.2]. But $\tilde{A} = A_\theta$, where A_θ is as given in Definition A1. Thus, the induced realization for $F_l(F, K)$ is stabilizable and detectable. In fact, since A_θ is Hurwitz (meaning that the system in Figure A2 is internally stable), we also know that $F_l(F, K) \in \mathscr{RH}_\infty$ (see [32, Lemma 12.2]).

DOI: 10.1002/rnc

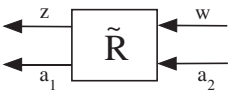

Figure A3. Input–output representation of $\tilde{R}$.

Figure A4. Chain-scattering representation of $\tilde{R}$.

A.2. $A_{F_1}+B_{F_1}F_{F_1}$ is Hurwitz

The proof of Lemma 4 requires us to show that the matrix denoted as $A_{F_1}+B_{F_1}F_{F_1}$ is Hurwitz. First, a review of the chain-scattering representation of a system, particularly $\tilde{R}$ as defined in (6), is required. Recall the input–output representation of $\tilde{R}$:

$$\begin{pmatrix} z \\ a_1 \end{pmatrix} = \tilde{R} \begin{pmatrix} w \\ a_2 \end{pmatrix} \tag{A8}$$

as shown in Figure A3. Since $(\tilde{R}_{21})^{-1}$ exists and is proper, (A8) can be alternatively represented as

$$\begin{pmatrix} z \\ w \end{pmatrix} = \mathrm{CHAIN}(\tilde{R}) \begin{pmatrix} a_2 \\ a_1 \end{pmatrix} \tag{A9}$$

where

$$\mathrm{CHAIN}(\tilde{R}) := \begin{pmatrix} \tilde{R}_{12}-\tilde{R}_{11}(\tilde{R}_{21})^{-1}\tilde{R}_{22} & \tilde{R}_{11}(\tilde{R}_{21})^{-1} \\ -(\tilde{R}_{21})^{-1}\tilde{R}_{22} & (\tilde{R}_{21})^{-1} \end{pmatrix}$$

Relation (A9) is referred to as the chain-scattering representation of $\tilde{R}$, as shown in Figure A4. A state-space representation for $\mathrm{CHAIN}(\tilde{R})$ is

$$\left(\begin{array}{c|cc} A_{\tilde{R}}-\dfrac{1}{\sqrt{\gamma^2-1}}B_{\tilde{R}_1}C_{\tilde{R}_2} & B_{\tilde{R}_2} & \dfrac{1}{\sqrt{\gamma^2-1}}B_{\tilde{R}_1} \\ \hline C_{\tilde{R}_1} & I & 0 \\ -\dfrac{1}{\sqrt{\gamma^2-1}}C_{\tilde{R}_2} & 0 & \dfrac{1}{\sqrt{\gamma^2-1}}I \end{array}\right) \tag{A10}$$

(refer to [41, Chapter 4.2] for the general state-space formula for CHAIN(·)).

Now $\mathrm{CHAIN}(\tilde{R}) \in \mathscr{RH}_\infty$ since

$$\mathrm{CHAIN}(\tilde{R}) = \begin{pmatrix} 0 & I \\ I & 0 \end{pmatrix} \mathrm{CHAIN}(R) \begin{pmatrix} 0 & I \\ I & 0 \end{pmatrix}$$

DOI: 10.1002/rnc

and CHAIN$(R) \in \mathscr{RH}_\infty$ [34]. Furthermore, (A10) is stabilizable and detectable since there exist matrices

$$\bar{F} := \begin{pmatrix} -C_{\tilde{R}_1} \\ C_{\tilde{R}_2} \end{pmatrix} \quad \text{and} \quad \bar{L} := (-B_{\tilde{R}_2} \;\; -B_{\tilde{R}_1})$$

such that

$$\bar{A} + \begin{pmatrix} B_{\tilde{R}_2} & \dfrac{1}{\sqrt{\gamma^2-1}} B_{\tilde{R}_1} \end{pmatrix} \bar{F} \quad \text{and} \quad \bar{A} + \bar{L} \begin{pmatrix} C_{\tilde{R}_1} \\ -\dfrac{1}{\sqrt{\gamma^2-1}} C_{\tilde{R}_2} \end{pmatrix}$$

respectively, are Hurwitz, where $\bar{A} := A_{\tilde{R}} - (1/\sqrt{\gamma^2-1}) B_{\tilde{R}_1} C_{\tilde{R}_2}$ (see Footnote ‖). Therefore, $\bar{A}$ is Hurwitz. However,

$$A_{F_1} + B_{F_1} F_{F_1} = \begin{pmatrix} \bar{A} & \bullet \\ 0 & A_{P_1} + B_{P_1} F_{P_1} \end{pmatrix}$$

where $\bullet$ denotes a 'do not care' element; hence, $A_{F_1} + B_{F_1} F_{F_1}$ is Hurwitz.

ACKNOWLEDGEMENTS

The authors gratefully acknowledge the contribution of Miss Lilangie Perera who coded the solution algorithm in Matlab. This work was supported by an ARC Discovery-Projects Grant (DP0342683) and National ICT Australia. National ICT Australia is funded through the Australian Government's *Backing Australia's Ability* initiative, in part through the Australian Research Council.

REFERENCES

1. Boyd S, Yang Q. Structured and simultaneous Lyapunov functions for system stability problems. *International Journal of Control* 1989; **49**(6):2215–2240.
2. Packard A, Doyle J. Quadratic stability with real and complex perturbations. *IEEE Transactions on Automatic Control* 1990; **35**(2):198–201.
3. Jönsson U, Rantzer A. Systems with uncertain parameters—time-variations with bounded derivatives. *International Journal of Robust and Nonlinear Control* 1996; **6**(9–10):969–982.
4. Megretski A. Frequency-domain criteria of robust stability for slowly time-varying systems. *IEEE Transactions on Automatic Control* 1995; **40**(1):153–155.
5. Braatz RD, Morari M. On the stability of systems with mixed time-varying parameters. *International Journal of Robust and Nonlinear Control* 1997; **7**:105–112.
6. Doyle JC. Analysis of feedback systems with structured uncertainties. *IEE Proceedings*, *Part D* 1982; **129**(6): 242–250.
7. Doyle JC, Wall JE, Stein G. Performance and robustness analysis for structured uncertainty. *Proceedings of the 21st IEEE Conference on Decision and Control*, Orlando, FL, U.S.A., 1982; 629–636.
8. Doyle JC. Structured uncertainty in control system design. *Proceedings of the 24th IEEE Conference on Decision and Control*, Fort Lauderdale, FL, U.S.A., 1985; 260–265.
9. VanAntwerp JG, Braatz RD, Sahinidis NV. Globally optimal robust process control. *Journal of Process Control* 1999; **9**:375–383.
10. Fukuda M, Kojima M. Branch-and-cut algorithms for the bilinear matrix inequality eigenvalue problem. *Computational Optimization and Applications* 2001; **19**:79–105.
11. Khammash M, Salapaka MV, Van Voorhis T. Robust synthesis in l_1: a globally optimal solution. *IEEE Transactions on Automatic Control* 2001; **46**(11):1744–1754.

DOI: 10.1002/rnc

12. Shamma J. Robust stability with time-varying structured uncertainty. *IEEE Transactions on Automatic Control* 1994; **39**(4):714–724.
13. Dullerud GE, Paganini F. *A Course in Robust Control Theory*: *A Convex Approach*. Springer: New York, 2000.
14. Dahleh MA, Diaz-Bobillo IJ. *Control of Uncertain Systems*: *A Linear Programming Approach*. Prentice-Hall: Englewood Cliffs, NJ, 1995.
15. Glover K, McFarlane D. Robust stabilization of normalized coprime factor plant descriptions with $\mathscr{H}_\infty$-bounded uncertainty. *IEEE Transactions on Automatic Control* 1989; **34**(8):821–830.
16. Qiu L, Davison EJ. Feedback stability under simultaneous gap metric uncertainties in plant and controller. *Systems and Control Letters* 1992; **18**:9–22.
17. Vinnicombe G. *Uncertainty and Feedback*: $\mathscr{H}_\infty$ *Loop-shaping and the v-gap Metric*. Imperial College Press: London, 2001.
18. Vinnicombe G. Frequency domain uncertainty and the graph topology. *IEEE Transactions on Automatic Control* 1993; **38**(9):1371–1383.
19. El-Sakkary AK. The gap metric: robustness of stabilization of feedback systems. *IEEE Transactions on Automatic Control* 1985; **30**(3):240–247.
20. Georgiou TT. On the computation of the gap metric. *Systems and Control Letters* 1988; **11**:253–257.
21. Georgiou TT, Smith MC. Optimal robustness in the gap metric. *IEEE Transactions on Automatic Control* 1990; **35**(6):673–685.
22. Gough NE, El-Sakkary AK. Basic procedure for model comparison using the gap metric. *International Journal of Systems Science* 1985; **16**(5):589–604.
23. Zhu SQ, Hautus MLJ, Praagman C. Sufficient conditions for robust BIBO stabilization: given by the gap metric. *Systems and Control Letters* 1988; **11**:53–59.
24. Georgiou TT, Pascoal A, Khargonekar PP. On the robust stabilizability of uncertain linear time-invariant plants using nonlinear time-varying controllers. *Automatica* 1987; **35**(5):617–624.
25. Georgiou TT. Differential stability and robust control of nonlinear systems. *Mathematics of Control*, *Signals*, *and Systems* 1993; **6**:289–306.
26. Georgiou TT, Smith MC. Robustness analysis of nonlinear feedback systems: an input–output approach. *IEEE Transactions on Automatic Control* 1997; **42**(9):1200–1221.
27. Feintuch A. The gap metric for time-varying systems. *Systems and Control Letters* 1991; **16**:277–279.
28. James MR, Smith MC, Vinnicombe G. Gap metrics, representations, and nonlinear robust stability. *SIAM Journal on Control and Optimization* 2005; **43**(5):1535–1582.
29. Vinnicombe G. On IQCs and the ν-gap metric. *Proceedings of the 37th IEEE Conference on Decision and Control*, Tampa, FL, U.S.A., 1998; 1199–1200.
30. Vinnicombe G. A ν-gap distance for uncertain and nonlinear systems. *Proceedings of the 38th IEEE Conference on Decision and Control*, Phoenix, AZ, U.S.A., 1999; 2557–2562.
31. Anderson BDO, Brinsmead TS, De Bruyne F. The Vinnicombe metric for nonlinear operators. *IEEE Transactions on Automatic Control* 2002; **47**(9):1450–1465.
32. Zhou K, Doyle JC, Glover K. *Robust and Optimal Control*. Prentice-Hall: Upper Saddle River, NJ, 1996.
33. Green M, Limebeer DJN. *Linear Robust Control*. Prentice-Hall: Englewood Cliffs, NJ, 1995.
34. Cantoni M, Vinnicombe G. Controller discretisation: a gap metric framework for analysis and synthesis. *IEEE Transactions on Automatic Control* 2004; **49**(11):2033–2039.
35. Cantoni M. On model reduction in the ν-gap metric. *Proceedings of the 40th IEEE Conference on Decision and Control*, Orlando, FL, U.S.A., 2001; 3665–3670.
36. Cantoni M, Vinnicombe G. Controller discretisation: a gap metric framework for analysis and synthesis. *Technical Report TR04-04*, Department of Electrical and Electronic Engineering, The University of Melbourne, 2004.
37. Vinnicombe G. On closed-loop objectives and guaranteed robustness properties. *Proceedings of the 35th IEEE Conference on Decision and Control*, Kobe, Japan, 1996; 1869–1874.
38. Lanzon A. Weight optimization in $\mathscr{H}_\infty$ loop-shaping. *Automatica* 2005; **41**:1201–1208.
39. McFarlane D, Glover K. A loop shaping design procedure using $\mathscr{H}_\infty$ synthesis. *IEEE Transactions on Automatic Control* 1992; **37**(6):759–769.
40. Papageorgiou G, Glover K. Design, development and control of the HIRM wind tunnel model. *Proceedings of the 38th IEEE Conference on Decision and Control*, vol. 2, Phoenix, AZ, U.S.A., 1999; 1529–1537.
41. Kimura H. *Chain-scattering Approach to* $\mathscr{H}^\infty$*-control*. Birkhäuser: Boston, Cambridge, MA, 1997.

DOI: 10.1002/rnc